Supplementary information

Selective Blockade of Neuronal BK (α+β4) Channel Preventing Epileptic Seizure

Xinlian Liu[1,4,§], Jie Tao[2,3,§], Shuzhang Zhang[3], Wenxian Lan[1], Chunxi Wang[1], Yonghua Ji[3,5,*], Chunyang Cao[1,4,6*]

[1] State Key Laboratory of Bioorganic and Natural Product Chemistry, Center for Excellence in Molecular Synthesis, Shanghai Institute of Organic Chemistry, Chinese Academy of Sciences, 345 Lingling Road, Shanghai, 200032, China. [2] Central Laboratory, Putuo Hospital, Shanghai University of Traditional Chinese Medicine, 164 Lanxi Road, Putuo District, Shanghai, 200062, China. [3] Institute of Biomembrane and Biopharmaceutics, Shanghai University, 99 Shangda Road, BaoShan District, Shanghai, 200444, China. [4] University of Chinese Academy of Science, No. 19A, Yuquan Road, Shijingshan District, Beijing, 100049, China. [5] Xinhua Hospital (Chongming) Affiliated to Shanghai JiaoTong University School of Medicine, Shanghai Chongming Xinhua Translational Medical Institute for Cancer Pain, 25 Nanmen Port Street, Chongming Branch, Shanghai, 202150, China.[6]Institute of Drug Discovery Technology, Ningbo University, No 818 Fenghua Road, Ningbo, Zhejiang, 313211, China.

Contents:

Preparation and characterization of recombinant MarTX, and its inhibitory effects on BK (α+β4) channels

Martentoxin (MarTX) is a 37-residue peptide, originally purified from the venom of the East-Asian scorpion (*Buthus martensi Karsch*), containing a triple-stranded antiparallel β-sheet anchored to a single α-helix by three disulfide bridges (Cys^{8}-Cys^{29}, Cys^{14}-Cys^{34}, and Cys^{18}-Cys^{36}) (Fig S1a). Purification of MarTX from its native source is costly and yields only a small amount of the peptide. Moreover, MarTX contains three disulfide bonds, which results in easy generation of inclusion bodies during over-expression in *E coli* system. We here produced large quantities of genetically operable MarTX with a plasmid, whose integrality and folding were confirmed by MALDI-TOF mass spectrum and one-dimensional (1D) ^{1}H nuclear magnetic resonance (NMR) spectrum, respectively (Fig S1b and S1c). To probe whether this recombinant MarTX (rMarTX) has a global folding similar to that of native form, we further determined its solution structure mainly using 364 NOE-derived distance constrains through program XPLOR-NIH [1], which has a backbone-atom RMSD of 1.27Å to the structure of native MarTX (pdb code 1M2S) [2] by superimposing the backbone atoms in secondary structure regions (Fig S2).

Human BK (α+β4) channel was expressed in HEK293T cells in order to investigate the pharmacological activity of rMarTX. The currents evoked by BK (α+β4) channel were measured at +80 mV with typical characteristics as reported [3-4]. The rMarTX peptide at 10 μM dose potently inhibited the currents (with the fraction of unlocked K^{+} current, $I_f^{rMarTX\text{-}WT}$ = 0.33 ± 0.06, Fig S1d and Table S1), which was close to the

inhibitory effect of native MarTX at 1 μM [4]. The dose response curve was obtained and the I_f was shown as a function of rMarTX concentration (Fig S1e). The IC_{50} value of rMarTX on BK (α+β4) channel was assessed to be 602 ±18 nM, with the Hill coefficient 1.60 ± 0.06. Taken together, the rMarTX has a similar global folding and close inhibitory activity to BK (α+β4) channel to that of its native form.

rMarTX interacts with the extracellular loop of human BK β4 subunit

As shown in Fig S1f, human BK β4 subunit contains two transmembrane domains (TM1 and TM2) and one extracellular loop (*i.e.*, hβ4-loop, *KCNMB4*, GenBank accession no. AF207992.1, 45-166 aa). Our recently reported NMR solution structure of hβ4-loop demonstrates that it contains two α-helices (α1 and α2), seven antiparallel β-sheets (β1, β2, β3, β4, β5, β6 and β7) and eight loops (L1, L2, L3, L4, L5, L6, L7 and L8), which are arranged in the order of β1- L1- β2-L2- β3-L3- β4- L4- β5- L5- α1- L6- α2- L7- β6- L8- β7 [3]. This structure is valuable for us to probe its potential interactions with rMarTX. The rMarTX peptide was titrated into ^{15}N-labeled hβ4-loop solution at mole ratios (hβ4-loop *vs* rMarTX) of 1:0, 1:0.3, 1:0.5, 1:1, 1:2 and 1:4, respectively, and then ^{1}H-^{15}N HSQC spectra were acquired. The cross-peaks in ^{1}H-^{15}N HSQC spectrum of ^{15}N-labeled hβ4-loop mixed with rMarTX at a mole ratio 1:2 (hβ4-loop vs rMarTX) were identical to those at a mole ratio 1:4, suggesting that the complex sample made at a mole ratio 1:2 was suitable for further structural analysis. Subsequently, we found that titration rMarTX into ^{15}N-labeled hβ4-loop solution resulted in very slight chemical shift perturbations of amide protons and nitrogen atoms of hβ4-loop (Fig S1g),

indicating that rMarTX weakly binds to hβ4-loop. Through microscale thermophoresis (MST), the binding affinity (K_D) of rMarTX to hβ4-loop was then measured as 511.05 ± 27.46 μM (Fig 1a), consistent with the results of NMR titration experiments.

Using ^{13}C, ^{15}N isotope double labeled hβ4-loop mixed with unlabeled rMarTX (hβ4-loop *vs* rMarTX = 1:2), we performed a series of three-dimensional (3D) NMR experiments and two-dimensional (2D) ^{13}C, ^{15}N edited filtered ^{1}H-^{1}H NOESY and TOCSY experiments, and we successfully assigned NMR signals of 92% backbone and 69% sidechain atoms of bound hβ4-loop, and most protons in bound rMarTX. Then ^{15}N-edited or ^{13}C edited HSQC-NOESY spectra with and without ^{15}N or ^{13}C decoupling during acquisition were acquired to distinguish intermolecular NOEs from intramolecular NOEs (Fig S3) [5]. Theoretically, in ^{15}N- or ^{13}C edited NOESY spectra with ^{15}N- or ^{13}C decoupling, all NOE cross-peaks are singlets, while in ^{15}N- or ^{13}C edited NOESY spectra without ^{15}N or ^{13}C decoupling, the intramolecular NOE cross-peaks split into two peaks, the intermolecular NOE cross-peaks are still singlets. Through this technique, we clearly got 35 intermolecular NOEs between rMarTX and hβ4-loop. Interestingly, the residues in rMarTX having intermolecular NOEs with hβ4-loop were found distributed around the peptide, not locating on a single region. In contrast, the residues in hβ4-loop displaying intermolecular NOEs with rMarTX mainly located on a single region (α-helix α1 plus loop L6, from Leu^{100} to Gln^{126}). These observations implied that one molecular rMarTX might interact with several hβ4-loop molecules.

However, we failed to get an exact mole ratio of rMarTX *vs* hβ4-loop directly

through isothermal titration calorimetry (ITC). But during our NMR signals assignments, only one set of NMR signals of hβ4-loop were observed, suggesting that different hβ4-loop molecules might encircle symmetrically around rMarTX. In addition, BKα channel is composed of pore-forming tetramer [6-9]. It was reported that BKα channel was expressed in neuron cell with BK β4 subunit at a mole ratio 1:1 [10]. Therefore, four identical BK β4 subunits may work together with four BKα subunits. MarTX was reported to specifically block K^+ currents of neuronal BK (α+β4) channel through sealing the pore [4]. Thus, we supposed that rMarTX could interact with hβ4-loop possibly at a mole ratio of 1: 4 (rMarTX *vs* hβ4-loop).

Construction of structural model of hβ4-loop in complex with rMarTX

We then constructed a structural model of four hβ4-loop molecules in complex with one molecular rMarTX (Fig 2a and 2b) through program XPLOR-NIH (NIH 2.47 version) using 9279 NOE-derived distance constraints (including 35 intermolecular NOEs), 664 dihedral angels for backbone ϕ and ψ angles and 328 hydrogen bonds (Table S3). A best-fit superposition of the ensemble of the 20 lowest-energy structures was displayed with the root mean square deviation (RMSD) values of 0.96 ± 0.11 Å for global backbone atoms and 1.53 ± 0.11 Å for global heavy atoms. The RMSD values were 0.54 ± 0.12 Å for the backbone (N, Ca and CO) atoms and 0.92 ± 0.12 Å for all heavy atoms in the well-ordered second structure regions. The *Ramachandran* plot displayed 78.3% of the residues in the most-favored regions and 14.0% residues in additionally allowed regions (Table S3), indicating the solution structures are

reasonable. As shown in Fig 2, four hβ4-loops (hereinafter, for simplicity, termed as monomers A, B, C and D, respectively) also form a rectangular pore, one molecular rMarTX locates in the central pore through hydrogen-bonds interactions with hβ4-loop. The interactions between rMarTX and hβ4-loop do not induce changes in global folding of rMarTX and hβ4-loop, with backbone-atom RMSD values of 1.08 Å and 1.83 Å, respectively, compared to their structures in free states (Fig S6).

Analysis of the results of chemical cross-linking assay

To double check the interfaces between rMarTX and hβ4-loop, we performed chemical cross-linking of proteins coupled with mass spectrometry analysis (CXMS) [11-12]. For comparison, we conducted three chemical cross-linking reactions. To test whether identical hβ4-loop molecules could be linked by cross-linking reagent, only hβ4-loop was used to react with the optimized concentration of disuccinimidyl suberate (*i.e.*, DSS, a N-hydroxysuccinimide ester (NHS ester), which reacts efficiently with primary amines in the side chain of lysine (K) residues and the N-terminus of each polypeptide, Fig S4a). Similarly, to test whether identical rMarTX molecules could be coupled by DSS, only rMarTX was selected to react with DSS. To check whether rMarTX and hβ4-loop could be linked by DSS, the complex of rMarTX and hβ4-loop (mole ratio = 2:1) was utilized to react with DSS. Before in-solution tryptic proteolysis, SDS_PAGE gel was run on all reaction reagents. As shown in Fig S4b, two hβ4-loops were linked by DSS, one hβ4-loop and one rMarTX were linked by DSS, and two hβ4-loops and one rMarTX were linked by DSS in solution. Then, the product of hβ4-loop

coupled with rMarTX by DSS was proteolyzed, which provided a mixture of three kinds of peptides inter-links, loop-links and mono-links [13]. All these peptides were subjected to LC-MS/MS (Fig S5), which demonstrated that DSS successfully linked the -NH_2 group of Lys^{120} in hβ4-loop with that of Lys^{28} in rMarTX, as well as that of Lys^{120} with the N-terminal -NH_2 group of the residue Gly^{-2} in rMarTX. As we know, the DSS spacer arm is about 11.4Å (Fig S4a). In our 20 structural models with the lowest energy, the average distances between the sidechain -NH_2 groups of Lys^{120} in hβ4-loop monomer A and of Lys^{28} in rMarTX are about 10.26 ± 0.99Å, and the distance between the sidechain -NH_2 groups of Lys^{120} of hβ4-loop monomer C and the N-terminal -NH_2 of residue Gly of rMarTX is 7.86 ± 1.44 Å, all of which are within the spacer arm of DSS. Therefore, the results from CXMS present the evidences of the interfaces existing between rMarTX and hβ4-loop monomers A or C.

Supporting references

1. Kuszewski, J.; Clore, G. M. Sources of and solutions to problems in the refinement of protein NMR structures against torsion angle potentials of mean force. *J. Magn. Reson.* 2000, *146*, 249-254.

2. Wang, Y.; Chen, X.; Zhang, N.; Wu, G.; Wu, H. The solution structure of BmTx3B, a member of the scorpion toxin subfamily alpha-KTx 16. *Proteins* 2005, *58*, 489-497.

3. Wang, Y.; Lan, W.; Yan, Z.; Gao, J.; Liu, X.; Wang, S.; Guo, X.; Wang, C.; Zhou, H.; Ding, J.; Cao, C. Solution structure of extracellular loop of human beta4 subunit of BK channel and its biological implication on ChTX sensitivity. *Sci*. *Rep*. 2018, *8*, 4571.

4. Shi, J.; He, H. Q.; Zhao, R.; Duan, Y. H.; Chen, J.; Chen, Y.; Yang, J.; Zhang, J. W.;

Shu, X. Q.; Zheng, P.; Ji, Y. H. Inhibition of martentoxin on neuronal BK channel subtype (alpha+beta4): implications for a novel interaction model. *Biophys*. *J*. 2008, *94*, 3706-3713.

5. Boetzel, R.; Czisch, M.; Kaptein, R.; Hemmings, A. M.; James, R.; Kleanthous, C.; Moore, G. R. NMR investigation of the interaction of the inhibitor protein Im9 with its partner DNase. *Protein Sci*. 2000, *9*, 1709-1718.

6. Wu, Y.; Yang, Y.; Ye, S.; Jiang, Y. Structure of the gating ring from the human large-conductance Ca(2+)-gated K(+) channel. *Nature* 2010, *466*, 393-397.

7. Yuan, P.; Leonetti, M. D.; Hsiung, Y.; MacKinnon, R. Open structure of the Ca^{2+} gating ring in the high-conductance Ca^{2+}-activated K^{+} channel. *Nature* 2011, *481*, 94-97.

8. Tao, X.; Hite, R. K.; MacKinnon, R. Cryo-EM structure of the open high-conductance Ca^{2+}-activated K^{+} channel. *Nature* 2017, *541*, 46-51.

9. Hite, R. K.; Tao, X.; MacKinnon, R. Structural basis for gating the high-conductance Ca(2+)-activated K(+) channel. *Nature* 2017, *541*, 52-57.

10. Wu, R. S.; Chudasama, N.; Zakharov, S. I.; Doshi, D.; Motoike, H.; Liu, G.; Yao, Y.; Niu, X.; Deng, S. X.; Landry, D. W.; Karlin, A.; Marx, S. O. Location of the beta 4 transmembrane helices in the BK potassium channel. *J*. *Neurosci*. 2009, *29*, 8321-8328.

11. Sinz, A. Chemical cross-linking and mass spectrometry to map three-dimensional protein structures and protein-protein interactions. *Mass Spectrom. Rev.* 2006, *25*, 663-682.

12. Xiao, K.; Zhao, Y.; Choi, M.; Liu, H.; Blanc, A.; Qian, J.; Cahill, T. J.; Li, X.; Xiao,

Y.; Clark, L. J.; Li, S. Revealing the architecture of protein complexes by an orthogonal approach combining HDXMS, CXMS, and disulfide trapping. *Nat. Protoc.* 2018, *13*, 1403-1428.

13. Tan, D.; Li, Q.; Zhang, M. J.; Liu, C.; Ma, C.; Zhang, P.; Ding, Y. H.; Fan, S. B.; Tao, L.; Yang, B.; Li, X.; Ma, S.; Liu, J.; Feng, B.; Liu, X.; Wang, H. W.; He, S. M.; Gao, N.; Ye, K.; Dong, M. Q.; Lei, X. Trifunctional cross-linker for mapping protein-protein interaction networks and comparing protein conformational states. *Elife* 2016, *5*, e12509.

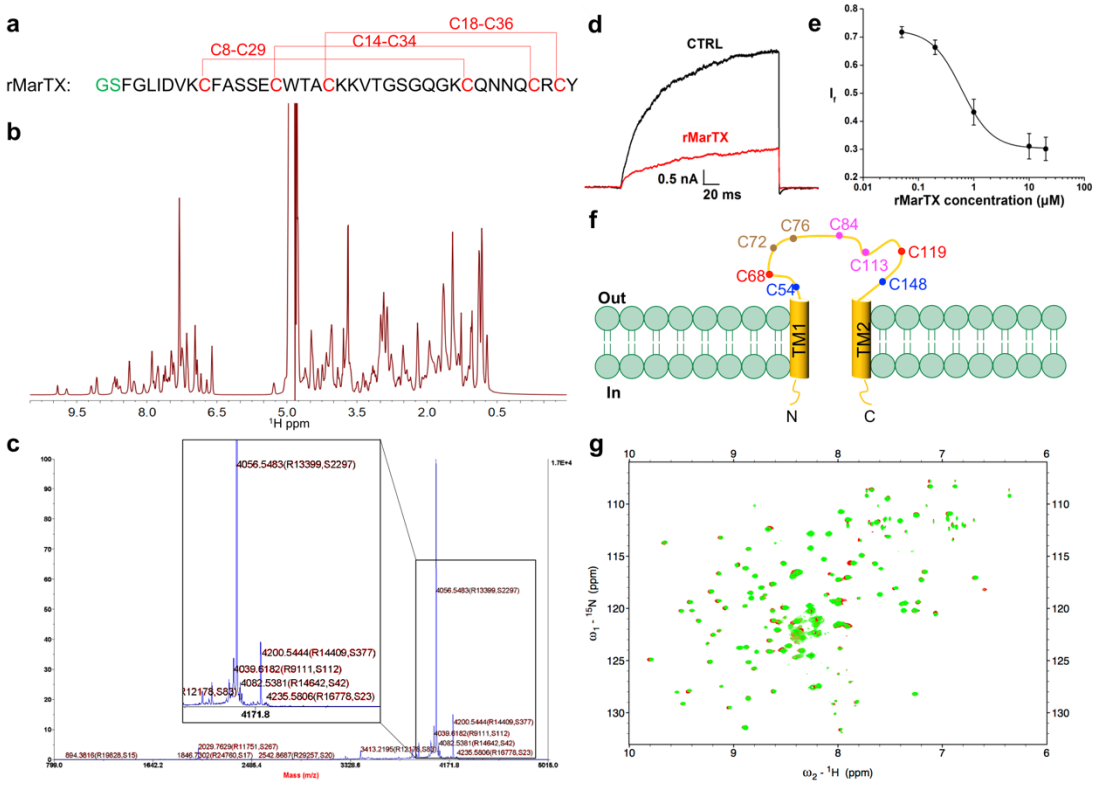

Figure S1. rMarTX preparation and characterization. (a) Sequence of rMarTX with three disulfide bonds. (b) 1D ^{1}H-NMR spectrum. (c) MALDI-TOF mass spectrum. (d) Representative whole cell current traces from HEK293T cells expressing human BKα and β4 subunits before and after the administration of 10 μM rMarTX. The holding voltage was −80 mV and the currents were elicited by a pulse of +80 mV with 300 nM free Ca^{2+} concentration in the pipette solution. (e) The dose-response curve of rMarTX inhibiting currents of BK(α+β4) channel was fitted by the Hill equation. Plot of the fraction of unblocked current (I_f) versus rMarTX concentration. Each point presented data from 5–8 cells. (f) The whole topology of human BK β4 subunit, in which the region of extracellular loop (*i.e.*, hβ4-loop, 45-166 aa, yellow line linked by TM1 and TM2) and cysteines forming disulfide bonds were highlighted. (g) Overlay of ^{1}H,^{15}N-HSQC spectra of 0.42 mM ^{15}N-labeled hβ4-loop before (red) and after (green) addition of 0.84 mM unlabeled rMarTX (hβ4-loop vs rMarTX = 1:2).

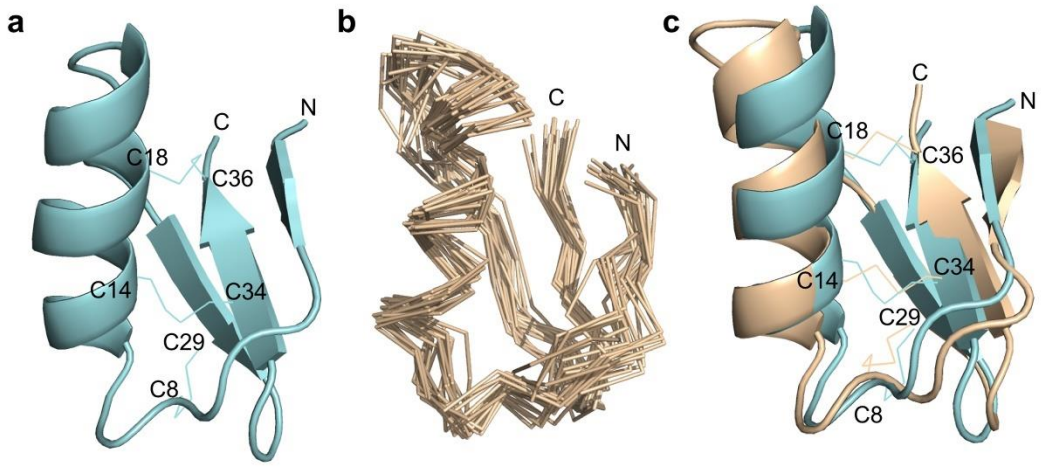

Figure S2. Structural comparison of rMarTX and native MarTX. (a) Solution structure of native MarTX (pdb code 1M2S)(in cyan). Disulfide bonds and the N- , C- termini were shown. (b) 20 structures of rMarTX with the lowest energy in wheat, only backbones were shown, the N- and C- termini were labeled. (c) Structural overlay of rMarTX (in wheat) and native MarTX (in cyan). RMSD = 1.27 Å. The disulfide bonds were highlighted, and the N-, C- termini were labeled.

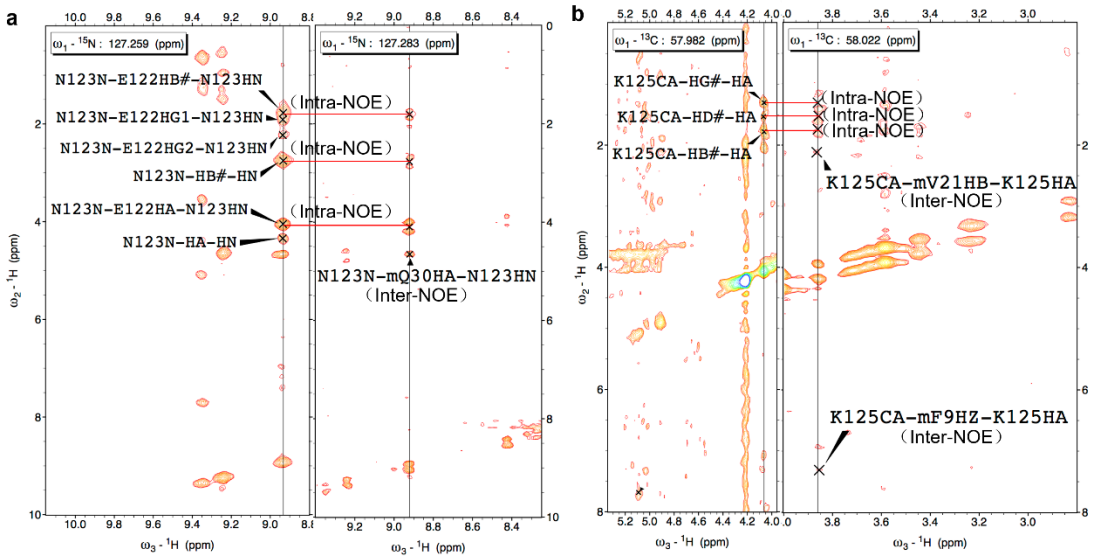

Figure S3. Intermolecular NOEs assignments based on the differences in the (a) ^{15}N-edited HSQC-NOESY spectra with and without ^{15}N decoupling and (b) in the ^{13}C edited HSQC-NOESY spectra with and without ^{13}C decoupling acquired on the ^{13}C, ^{15}N labeled hβ4-loop mixed with rMarTX (1:2). The results in a and b were just examples for understanding the assignment process of intermolecular NOEs.

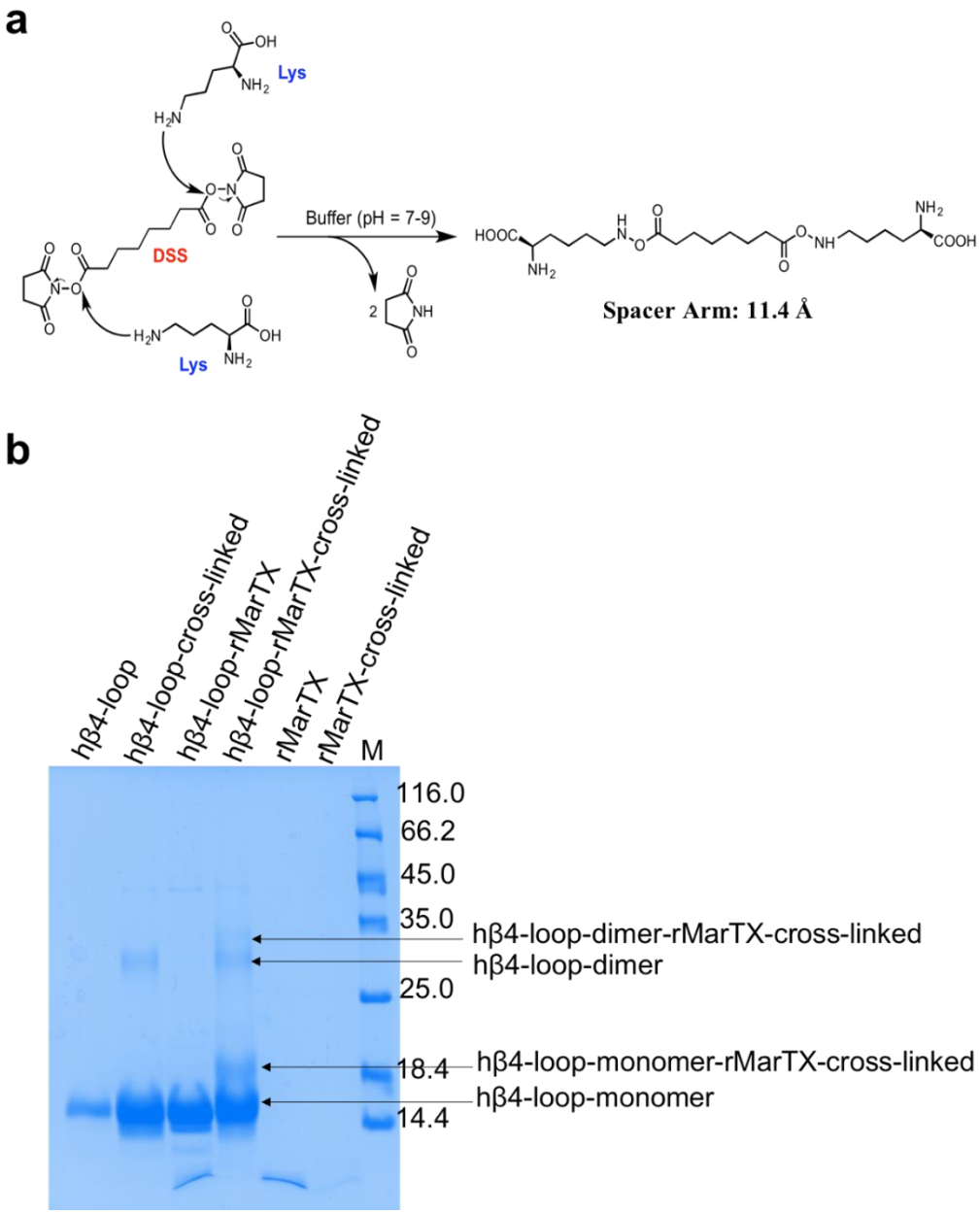

Figure S4. DSS-based cross-linking reactions between hβ4-loop and rMarTX. (a) The principle of DSS-based cross-linking reactions. DSS is a N-hydroxysuccinimide ester (NHS ester), and reacts efficiently with primary amines in the side chain of lysine (K) residues and the N-terminus of each polypeptide in pH 7 to 9 buffers to form stable amide bonds. The spacer arm is 11.4 Å. (b) SDS_PAGE gel were run on the reaction mixtures after the DSS-based chemical cross-linking reactions. Non-linked hβ4-loop and rMarTX were used as negative controls.

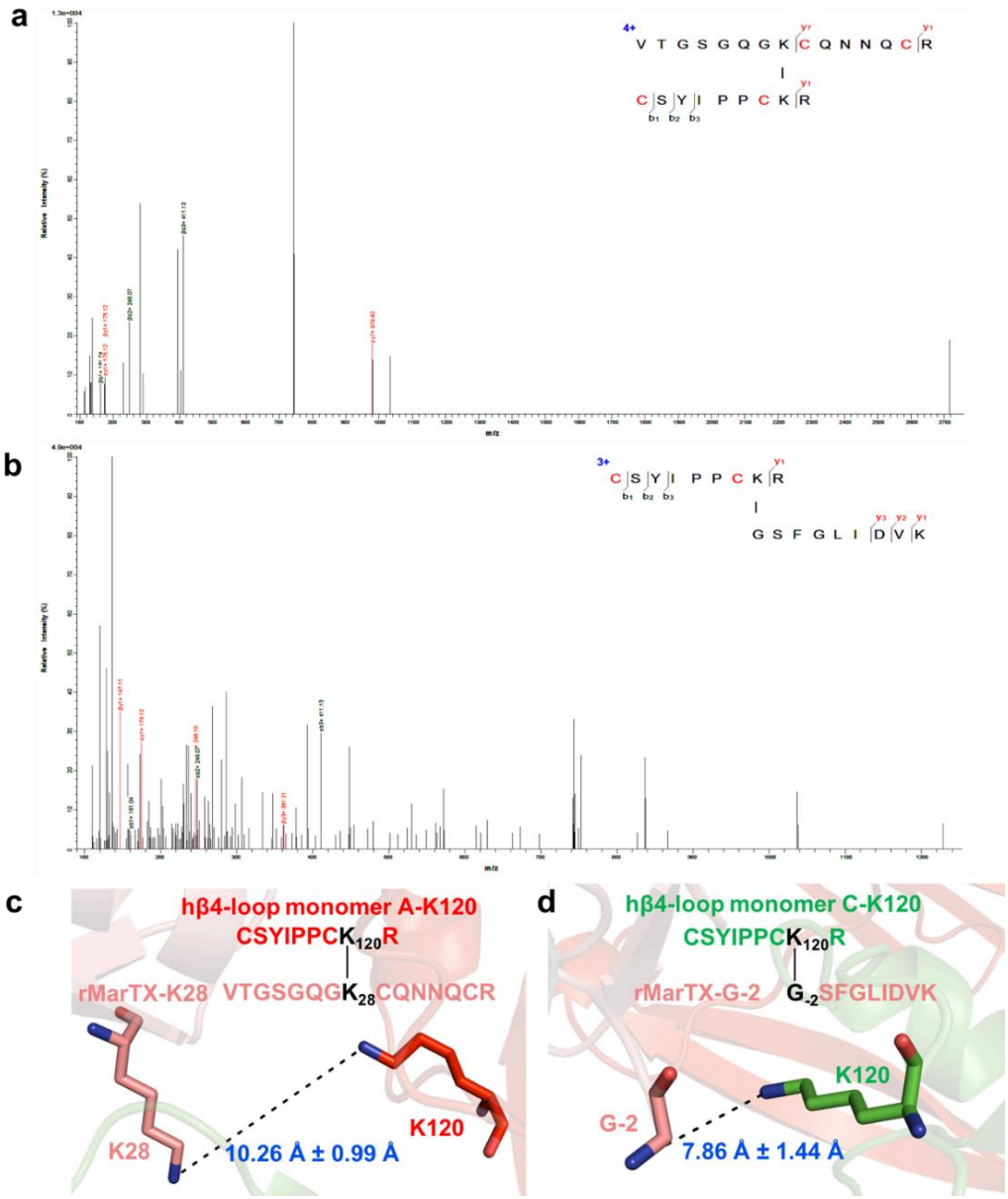

Figure S5. The interfaces between hβ4-loop and rMarTX were confirmed by DSS crosslinker-based CXMS analyses. (a, b) High resolution fragmentation spectra of the inter-linked peptides. Fragment peaks were annotated in red or green, y and b were shown as C-terminal and N-terminal fragment respectively, followed by the number of amino acids and the charge of the fragment. (c) The interface between hβ4-loop monomer A and rMarTX in the structural model was confirmed by intermolecular DSS cross-linking *in vivo* between hβ4-loop monomer A residue Lys^{120} and rMarTX residue Lys^{28}. (d) The interface between hβ4-loop monomer C and rMarTX in the structural model was confirmed by intermolecular DSS cross-linking *in vivo* between hβ4-loop monomer C residue Lys^{120} and rMarTX residue Gly^{-2}. The cross-linked residues were numbered and the calculated average distances between these $-NH_2$ groups in 20 structures were shown.

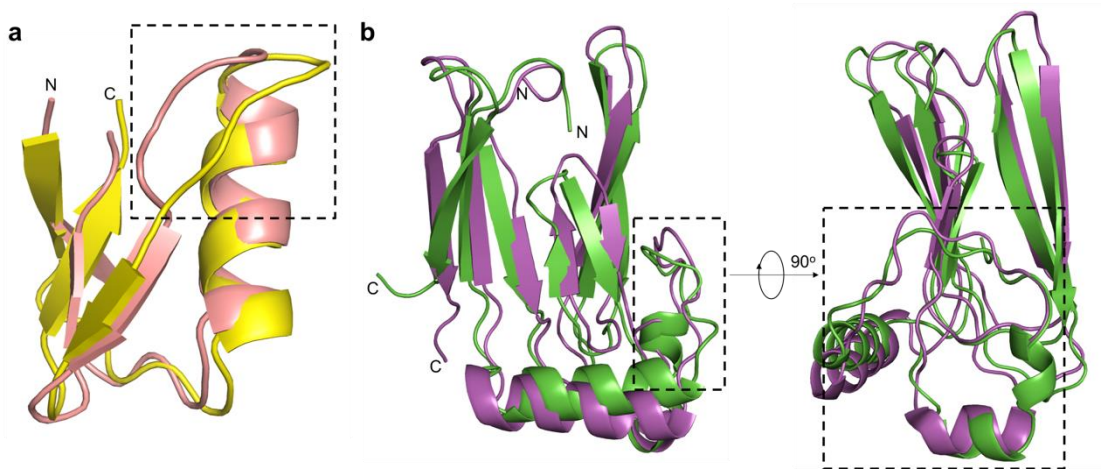

Figure S6. Interactions between hβ4-loop and rMarTX do not change the global folding of rMarTX and hβ4-loop. (a) Structure of bound rMarTX (in salmon) was overlapped with that of free MarTX (in yellow) through superimposing the backbone atoms in secondary structure regions of rMarTX. (b) Structure of free hβ4-loop (pdb code 5Y7L) (in magenta) was overlapped with that of rMarTX bound hβ4-loop in green through superimposing the backbone atoms in secondary structure regions. To clearly present the changes in the local conformation of the region from Leu^{100} to Gln^{126} of hβ4-loop upon its interacting with rMarTX, the orientation of the figure was rotated by 90°. In both a and b, the N- and C-termini of rMarTX or hβ4-loop were labeled. The dashed boxes indicated the local conformation changes in the loop (residues from Gly^{23} to Gln^{26}) of rMarTX and in the region of α-helix α1 and loop L6 of hβ4-loop.

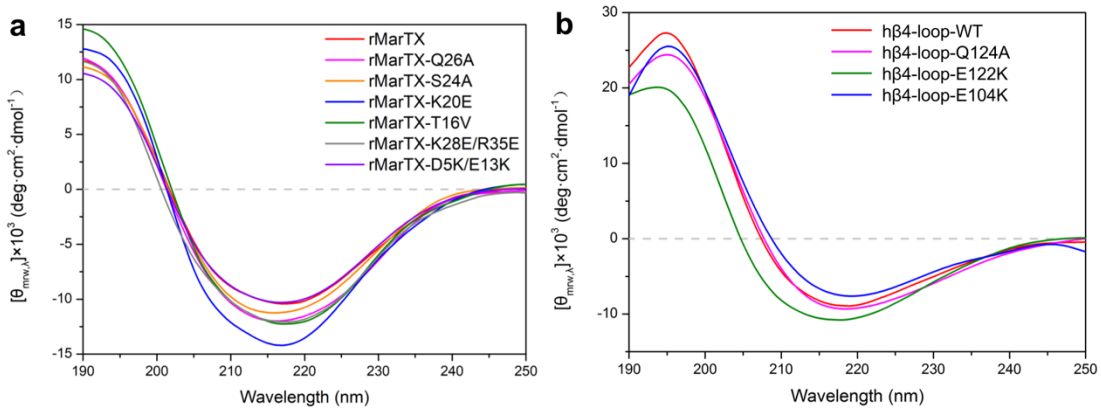

Figure S7. CD spectra of rMarTX, hβ4-loop and their variants.

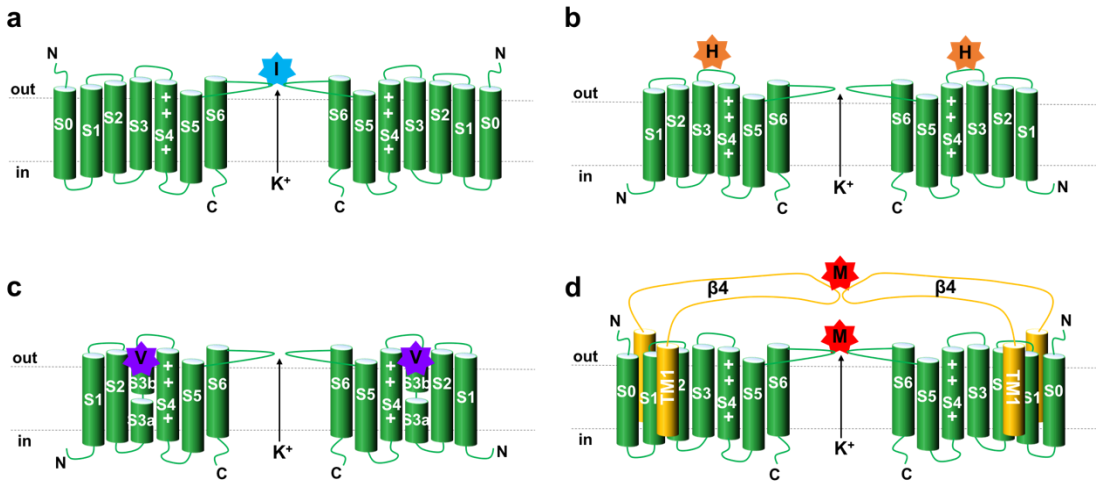

Figure S8. Different models for neurotoxins interacting with voltage-activated potassium channels suggested that MarTX interacts with BK (α+β4) channel in a novel way. (a) The scorpion toxin IbTX (abbreviated as I in cyan star) binds to the outer vestibule of the potassium conduction pore to block the BKα channel. (b) Hanatoxin (abbreviated as H in orange stars, separated from tarantula spider venom) modifies the gating of *drk1* voltage-activated K^+ channel through binding S3-S4 linker. (c) VsTX (abbreviated as V in purple stars, also separated from tarantula spider venom) exclusively binds on the voltage-sensor domain of voltage-dependent K^+ channel from *Aeropyrum pernix* (KvAP). The binding sites limit to the S3B segment of the voltage sensor. (d) MarTX (abbreviated as M in red stars) inhibit the BK(α+β4) channel through interactions with two pores formed by four extracellular loop of β4 subunit and by pore domains of α subunit.

Table S1. Pharmacological characterization of rMarTX or its variants on BK (α+β4) channel or its mutants.

Toxins	Channel	n	I_f (Fraction of currents)
rMarTX-WT	BK (α+β4)	6	0.33 ± 0.06
rMarTX-K20E	BK (α+β4)	7	0.80 ± 0.04***
rMarTX-T16V	BK (α+β4)	5	0.36 ± 0.03
rMarTX-S24A	BK (α+β4)	5	0.75 ± 0.08**
rMarTX-Q26A	BK (α+β4)	5	0.74 ± 0.03**
rMarTX-D5K/E13K	BK (α+β4)	4	0.56 ± 0.16
rMarTX-K28E/R35E	BK (α+β4)	5	0.80 ± 0.07***
rMarTX-WT	BK (α+β4 E104K)	5	0.94 ± 0.03***
rMarTX-WT	BK (α+β4 E122K)	4	0.88 ± 0.08***
rMarTX-WT	BK (α+β4 Q124A)	5	0.60 ± 0.08**
rMarTX-WT	BK (α+β4 E128K)	4	0.75 ± 0.12**

Note. ** $P< 0.01$; *** $P < 0.001$ compared to the group of BK (α+β4) channel treated with rMarTX-WT (One-way ANOVA).

Table S2. Intermolecular NOEs used in structural determination of hβ4-loop in complex with rMarTX.

Atom 1 (in rMarTX)	Atom 2 (in different hβ4-loop monomers)
F9 - Hδ	Monomer A - Y115 - Hα
F9 - Hε	Monomer A - H101 - Hα
F9 - Hζ	Monomer A - K125 - Hα
S12 – Hβ1	Monomer A - K125 - Hα
S12 – Hβ2	Monomer A - K125 - Hα
W15 - Hδ1	Monomer A - L127 –δ1-CH_3
W15 - Hδ1	Monomer A - L127 –δ2--CH_3
W15 - Hε1	Monomer A - L127 –δ1-CH_3
W15 - Hε1	Monomer A - L127 –δ2--CH_3
K20 – Hδ1	Monomer B - K125 - Hα
K20 – Hδ2	Monomer B - K125 - Hα
V21 - Hβ	Monomer B - K125 - Hα
G25 – Hα	Monomer B - K125 – Hβ1
G25 – Hα	Monomer B - K125 – Hβ2
I4 – Hγ1	Monomer B – L100 – δ1-CH_3
I4 – Hγ1	Monomer B – L100 – δ2--CH_3
Y37 - Hα	Monomer B - L100 –δ1-CH_3
Y37 - Hα	Monomer B - L100 –δ2--CH_3
F1 - Hδ	Monomer B - L100 –δ1-CH_3
F1 - Hδ	Monomer B - L100 –δ2--CH_3
Q30 - Hα	Monomer C - N123 - HN
R35 – Hβ1	Monomer C - K125 - Hα
R35 – Hβ2	Monomer C - K125 - Hα
Q26 – Hγ	Monomer C - K125 – Hβ1
Q26 – Hγ	Monomer C - K125 – Hβ2
E13 - Hα	Monomer C - K125 –Hγ1
E13 - Hα	Monomer C - K125 –Hγ2
D5 –Hβ	Monomer D - K125 – Hγ1
D5 –Hβ	Monomer D - K125 – Hγ2
C8 – Hβ	Monomer D - K125 – Hγ1
C8 –Hβ	Monomer D - K125 – Hγ2
I4 – Hβ	Monomer D - L127 –δ1-CH_3
I4 – Hβ	Monomer D - L127 –δ2--CH_3
V21 – Hβ	Monomer D - L127 –δ1-CH_3
V21 – Hβ	Monomer D - L127 –δ2--CH_3

Table S3. NMR structural constrains statistic used in determining structural model of hβ4-loop in complex with rMarTX. The programs PROCHECK and PROCHECK-NMR were used to check the overall quality of the structures. Gly and Pro were excluded from the *Ramachandran* analysis.

	hβ4-loop_rMarTX
Number of experimental restraints	
Distance restraints from NOEs	
Total	9279
Intra-residue(i-j=0)	3228
Sequential (|i-j|=1)	2836
Medium range (1<|i-j|≤5)	1392
Long range (|i-j|>5)	1788
Intermole	35
Hydrogen bonds	328
Dihedral angels	664
Structural statistics	
r.m.s.d versus the mean structure(Å)	
All backbone atoms	0.96 ± 0.11 Å
All heavy atoms	1.53 ± 0.11 Å
Backbone atoms(2nd structure)	0.54 ± 0.12 Å
Heavy atoms (2nd structure)	0.92 ± 0.12 Å
Rms Deviations from the experimental restraints	
NOE distances (Å)	0.030 ± 0.0015
Dihedral angles (deg.)	0.90 ± 0.071
Rms Deviations from idealized geometry	
Bonds (Å)	0.0018 ± 0.000057
Angles (deg.)	0.41 ± 0.0035
Impropers (deg.)	0.26 ± 0.0058
Ramachandran Analysis	
residues in most favored regions	78.3 %
residues in additionally allowed regions	14.0 %
residues in generously allowed regions	6.0 %
residues in disallowed regions	1.7 %

Table S4. Binding affinity data between hβ4-loop (or its variants) and rMarTX (or its variants) measured by MST.

Toxins	Protein	K_D (μM)
rMarTX-WT	hβ4-loop-WT	511.05 ± 27.46
rMarTX-T16V	hβ4-loop-WT	550.10 ± 20.03
rMarTX-Q26A	hβ4-loop-WT	639.70 ± 28.18
rMarTX-D5K/E13K	hβ4-loop-WT	1098.70 ± 3.11
rMarTX-S24A	hβ4-loop-WT	$(108.88 \pm 11.53)\times10^3$
rMarTX-K28E/R35E	hβ4-loop-WT	Not Detected
rMarTX-K20E	hβ4-loop-WT	Not Detected
rMarTX-WT	hβ4-loop-E104K	782.44 ± 80.11
rMarTX-WT	hβ4-loop-Q124A	974.89 ± 64.98
rMarTX-WT	hβ4-loop-E122K	Not Detected